

OXFORD CENTRE FOR COLLABORATIVE APPLIED MATHEMATICS

Report Number 09/47

Stochastic Partial Differential Equations as priors in ensemble methods for solving inverse problems

by

Roman V. Potsepaev, Chris L. Farmer, Mohammed Aziz



Oxford Centre for Collaborative Applied Mathematics
Mathematical Institute
24 - 29 St Giles'
Oxford
OX1 3LB
England

Stochastic Partial Differential Equations as priors in ensemble methods for solving inverse problems.

Roman V. Potsepaev*
Schlumberger Abingdon Technology Centre

Chris L. Farmer
OCCAM, University of Oxford

Mohammed Aziz
OCIAM, University of Oxford.

January 25, 2010

Abstract

This article describes a coordinate free approach to modelling stochastic textures through the application of stochastic partial differential equations. The intended application is that of sampling from a prior probability density in the solution of inverse problems by Bayesian filtering methods. In simpler cases analytical formulae for the correlation functions can be derived. Such formulae can then be used to guide parameter selection in the general case where numerical methods are necessary.

1 Introduction

Mathematical models are studied using computer simulation in almost all areas of applied and computational mathematics. Most such applications require the solution of inverse problems. The large and growing literature in areas such as weather forecasting, climate prediction and oil reservoir forecasting is of particular interest to the authors. In these problems the

*Corresponding author, RPotsepaev@slb.com.

prior information has specific geometric and visual qualities that need to be summarised in a mathematical way. The difficulties are severe in the geoscience applications involving complicated geometric features arising from sedimentary and tectonic processes that affect the spatial distribution of physical properties. However the need to summarise properties influenced by geometric complications arises in many inverse problems. For definiteness in the following, the focus is on the geoscience, petroleum reservoir problem. However we hope that the ideas and literature in the discussion will be of general interest and value.

Reservoir simulation models are widely used by oil and gas companies for production forecasts and for making investment decisions. In order to minimize the mismatch between simulated and observed measurements of production data the inverse problem, known as 'history matching' in petroleum engineering, needs to be solved. The solution of the inverse problem provides an estimate of the reservoir rock parameters such as permeability and porosity. Another approach is within a Bayesian formulation of the inverse problem and subsequent application of an Ensemble Kalman filter or other, more rigorous, sequential Monte Carlo method. The Ensemble Kalman Filter [7] is one of the most successful and popular approaches even though it makes assumptions of linearity in parts of the derivation. All of the ensemble methods, as does the basic Bayesian framework, require a prior to be specified.

The focus of this article is on stochastic sampling from a prior probability distribution, in other words, the generation of realizations of reservoir parameters based on assumptions regarding reservoir structure (geological layers and faults), the shape of the correlation function and a set of measurements made during well logging. An ensemble of such realizations serves as input for the Monte Carlo methods mentioned above. Modelling unknown functions in models is within the domain of spatial statistics or, as sometimes called, 'geostatistics'. In some cases the prior is specified as a closed form probability density function and in other cases by a stochastic process. In this paper we study a particular stochastic process - an elliptic stochastic partial differential equation (SPDE) - and derive the probability density function for special cases that are sufficient to guide the initial choice of parameters in the prior.

There are many texts on stochastic sampling, and we only give a concise overview and some selected references. A comprehensive overview of simulation methods in geostatistics can be found in [5]. The Metropolis-Hastings algorithm and sampling from a Langevin equation are widely used in statistical physics [3]. The Gibbs Sampler was introduced into the image processing literature by [11]. The distinctive feature of these methods is the

necessity to make many iterations before the realizations are suitable for use. However, in some methods such as the technique of sequential Gaussian simulation [5], a compromise is made and only a limited number of iterations are performed, perhaps only one, and the realizations form only an approximate ensemble from the target prior. In applications of geostatistics the method of sequential Gaussian simulation has achieved great popularity. Other methods for simulation of stochastic fields include: the LU-decomposition method, turning bands, the spectral representation method, and the Karhunen-Loève expansion [5, 6].

Existing geostatistical algorithms for stochastic simulation require a mapping, called a *uvt*-transform, from physical to parametric space resulting in a stratigraphic coordinate system. The parametric space can be considered to represent a pre-deformed and pre-faulted deposition environment. This method assumes that the property layering follows the original depositional layering thus ignoring later geological modification by, for example, diagenetic processes. After appropriate scaling to remove anisotropy in the correlation function, the reservoir properties are modelled in stratigraphic coordinates by, for example, a Gaussian stationary random field and then mapped back into the physical space. Due to the structural complexity of geological layers which might be twisted, pinched-out and faulted, the construction of the stratigraphic coordinate system is very hard to archive. Existing approximations of this coordinate system in many cases cause significant distortions in the correlation distances. The major advantage of the method we propose in this paper is that the stratigraphic coordinate system becomes unnecessary when Markov fields are generated as solutions of stochastic partial differential equation. This is analogous to the fact that when fluid flow, or other continuum processes are modelled in a local way, using a partial differential equation (PDE), then a global coordinate system that follows the geometry is unnecessary, and only a local coordinate system is required when performing calculations.

Whittle [19] and Heine [12] introduced stochastic partial differential equations to describe random fields and numerical procedures were subsequently developed to generate random realizations [2, 13] for stationary fields in a parametric space. In this paper we extend this approach and propose a method for sampling random fields directly in physical space in the presence of geological deformations and faults. We also provide a general mathematical framework for application of stochastic elliptic PDEs to random field generation. In particular we extend an existing method of white noise approximation and prove numerical convergence.

The paper is organized as follows. The next section provides an overview of a general theory of stochastic elliptic PDEs. In particular, the modified

Helmholtz equation driven by white noise and properties of its solution are discussed. Section 3 is devoted to the boundary value problem for stochastic PDEs and the dependency of the covariance function of its solution from the distance to the boundary. An approximation of 'white noise' is presented in Section 4 and we show that the solution of the equation with approximated white noise converges to the solution of the equation with analytical white noise. In section 5 the method for sampling directly in physical space is described in detail. Conditional simulation and the relation to Tikhonov regularization are discussed in section 6. Section 7 is devoted to the Biharmonic-Helmholtz equation and correlation functions of its solutions. Finally Section 8 contains some concluding remarks and perspectives for further work.

2 Theoretical framework.

2.1 Random fields.

A collection of random variables $\xi(x) \in L^2(\Omega, \mathcal{F}, P),\ x \in G$ dependent on a vector parameter x in a region $G \subseteq \mathbf{R}^d$ is called a *random field*. We consider real Gaussian random fields with zero mean $E[\xi(x)] = 0$ and finite variance $E[\xi(x)^2] < \infty$.

Consider the space $C_0^\infty(G)$ of infinitely differentiable functions $u = u(t), t \in G$ with compact support. The linear continuous operator which maps functions $u \in C_0^\infty(G)$ into $L^2(\Omega, \mathcal{F}, P)$

$$\xi = (u, \xi), \qquad u \in C_0^\infty(G),$$

is called a *generalized random field*. For $\xi = (u, \xi)$ differentiation is defined as for generalized functions, that is

$$D^k \xi = (-1)^{|k|}(D^k u, \xi).$$

As an example we consider the generalized random field associated with an ordinary random function $\xi(x),\ x \in G$

$$(u, \xi) = \int_G u(x)\xi(x)dx, \qquad u \in C_0^\infty(G). \tag{1}$$

Another important example is Gaussian "white noise" - the generalized random function in $G \subseteq \mathbf{R}^d$

$$\dot{\eta}(u) = \int_G u(x)\eta(dx), \qquad u \in C_0^\infty(G),$$

where $\eta(dx)$ is the Gaussian orthogonal measure, that is

$$E[\eta(\Delta)] = 0, \qquad E[\eta(\Delta_1)\eta(\Delta_2)] = \int_{\Delta_1 \cap \Delta_2} dx.$$

2.2 Stochastic Partial Differential Equations driven by white noise.

Consider an elliptic partial differential equation driven by Gaussian white noise

$$L\xi(u) = \dot{\eta}(u), \qquad u \in C_0^\infty(G), \tag{2}$$

where L is a uniformly elliptic and formally self-adjoint differential operator

$$Lu = \sum_{|\alpha|,|\beta| \le l/2} (-1)^{|\alpha|} D^\alpha [a_{\alpha\beta}(x) D^\beta u], \qquad u \in C_0^\infty(G) \tag{3}$$

with smooth bounded coefficients $a_{\alpha\beta}(\mathbf{x})$, $x \in G$. In the following we shall assume the existence of a square integrable Green's function $g(\mathbf{x}, \mathbf{y})$ for L in G; also we assume that

$$l > d/2, \tag{4}$$

where l is the order of the differential operator L and d is the dimension of the region $G \subseteq \mathbf{R}^d$.

The generalized field

$$\xi(u) = \dot{\eta}(L^{-1}u), \qquad u \in C_0^\infty(G)$$

is the unique solution of (2); if condition (4) is satisfied, than the solution of (2) is an ordinary Gaussian random field (see [16], theorem on p.533), i.e.

$$\xi(\mathbf{x}) = \int_{\mathbf{R}^d} g(\mathbf{x}, \mathbf{y}) \eta(d\mathbf{y}), \qquad \mathbf{x} \in G, \tag{5}$$

In addition, $\xi(\mathbf{x})$ is a Markov random field, which intuitively means that for any smooth surface Γ which separates G into complementary domains, what happens inside is independent of what happens outside when conditioned by knowledge of $\xi(\mathbf{x})$ on Γ and all derivatives $\xi^{(k)}(x)$, $x \in \Gamma$, $(1 \le k \le l-1)$ taken in the direction orthogonal to Γ (see [15], [16], [17] for details).

For the equation (2) we will often be using formal notation

$$L\xi(\mathbf{x}) = \dot{\eta}(\mathbf{x}), \qquad \mathbf{x} \in G, \tag{6}$$

with the same meaning as (2). Formally $\dot{\eta}(\mathbf{x})$ my be interpreted as an ordinary random field with

$$E[\dot{\eta}(\mathbf{x})] = 0, \qquad E[\dot{\eta}(\mathbf{x})\dot{\eta}(\mathbf{y})] = \delta(\mathbf{x} - \mathbf{y})$$

A special case of (3) is the operator

$$L = \sum_{i=0}^{m} a_i \nabla^{2i}. \tag{7}$$

In this special case the solution (5) is defined as the stochastic integral

$$\xi(\mathbf{x}) = \int_{\mathbf{R}^d} g(\|\mathbf{x}-\mathbf{y}\|)\eta(d\mathbf{y}), \qquad \mathbf{x} \in G, \tag{8}$$

where $g(\|\mathbf{x}-\mathbf{y}\|)$ is Green's function for L, i.e. $Lg(\|\mathbf{x}-\mathbf{y}\|) = \delta(\|\mathbf{x}-\mathbf{y}\|)$. The covariance function $E\left[\xi(\mathbf{x})\xi(\mathbf{y})\right]$ for this zero mean Gaussian field can be expressed as

$$C(\|\mathbf{x}-\mathbf{y}\|) = \int_{\mathbf{R}^d} g(\|\mathbf{x}-\mathbf{x_0}\|)g(\|\mathbf{y}-\mathbf{x_0}\|)d\mathbf{x_0} \tag{9}$$

therefore, the field is stationary.

Note also that the covariance function (9) represents Green's function for the operator L^2

$$L^2C(\|\mathbf{x}-\mathbf{y}\|) = \delta(\|\mathbf{x}-\mathbf{y}\|) \tag{10}$$

which immediately follows from

$$\begin{aligned} LC(\|\mathbf{x}-\mathbf{y}\|) &= \int_{\mathbf{R}^d} Lg(\|\mathbf{x}-\mathbf{x_0}\|)g(\|\mathbf{y}-\mathbf{x_0}\|)d\mathbf{x_0} \\ &= \int_{\mathbf{R}^d} \delta(\|\mathbf{x}-\mathbf{x_0}\|)g(\|\mathbf{y}-\mathbf{x_0}\|)d\mathbf{x_0} \\ &= g(\|\mathbf{x}-\mathbf{y}\|). \end{aligned}$$

The following theorem provides a useful tool to evaluate the covariance function from Green's function.

Theorem 2.1. *For the equation (5) with the operator defined as*

$$a_m\nabla^{2m} + a_{m-1}\nabla^{2m-2} + ... + a_0$$

the covariance function satisfies the equation

$$C(\|\mathbf{x}-\mathbf{y}\|) = -\frac{\partial g(\|\mathbf{x}-\mathbf{y}\|)}{\partial a_0}. \tag{11}$$

Proof. Writing $L\xi(\mathbf{x}) = \dot{\eta}(\mathbf{x})$, we have $Lg(\|\mathbf{x}-\mathbf{y}\|) = \delta(\|\mathbf{x}-\mathbf{y}\|)$.

Differentiating both sides by a_0 we obtain,

$$a_m\nabla^{2m}\frac{\partial g(\|\mathbf{x}-\mathbf{y}\|)}{\partial a_0} + a_{m-1}\nabla^{2m-2}\frac{\partial g(\|\mathbf{x}-\mathbf{y}\|)}{\partial a_0} + ... + a_0\frac{\partial g(\|\mathbf{x}-\mathbf{y}\|)}{\partial a_0} + g(\|\mathbf{x}-\mathbf{y}\|) = 0,$$

or

$$L\frac{\partial g(\|\mathbf{x}-\mathbf{y}\|)}{\partial a_0} = -g(\|\mathbf{x}-\mathbf{y}\|),$$

therefore

$$L^2\frac{\partial g(\|\mathbf{x}-\mathbf{y}\|)}{\partial a_0} = -Lg(\|\mathbf{x}-\mathbf{y}\|) = -\delta(\|\mathbf{x}-\mathbf{y}\|)$$

From (10) we obtain (11) □

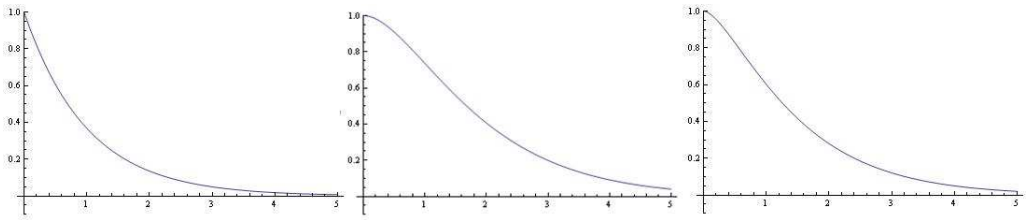


Figure 1: Correlation functions ($a = 1$) for $d = 1, 2, 3$.

2.3 Modified Helmholtz equation

The main instrument for generating random fields in the article is the modified Helmholtz equation,

$$-b\nabla^2\xi(x) + ba^2\xi(x) = \dot{\eta}(x), \quad x \in \mathbf{R}^d. \tag{12}$$

From now on, for brevity, we will simply call this equation 'Helmholtz equation'. Green's function, the covariance function and the correlation function (fig. 1) for this equation are: for $d = 1$

$$G(r) = \frac{e^{-ar}}{2ab}, \quad C(r) = \frac{(1+ar)e^{-ar}}{4a^3b^2}, \quad \rho(r) = (1+ar)e^{-ar};$$

for $d = 2$

$$G(r) = \frac{1}{2\pi b}K_0(ar), \quad C(r) = \frac{ar}{4\pi b^2a^2}K_1(ar), \quad \rho(r) = ar \cdot K_1(ar);$$

where the K's are the modified Bessel functions of the second kind; for $d = 3$

$$G(r) = \frac{e^{-ar}}{4\pi br}, \quad C(r) = \frac{e^{-ar}}{8\pi ab^2}, \quad \rho(r) = e^{-ar}.$$

3 Boundary value problems and distortion of the random field near the boundary.

If we are to use SPDE to generate samples from a prior on a *finite domain* then we must apply some boundary conditions. Of course, this is true whatever method we use to generate the random fields but when using an SPDE, at least in the elliptic case studied here, one has to be quite explicit about such conditions. If we were to frame the problem in a variational setting the question of boundary conditions would be somewhat hidden but we would

in fact be using the natural boundary conditions implied by the variational principle. In this section we are primarily concerned with showing what happens when one uses homogeneous Dirichlet or Neumann conditions. We will show that such conditions distort the correlation structure. Depending upon the intended application this might be a source of difficulty. As the domains are generally complicated and even non-convex the use of periodic conditions is not generally possible, and anyway would introduce correlation artefacts that could be harmful to the results. We discuss a practical approach at the end of this section.

The solution for the boundary value problem for equation (12) may be represented as

$$u(\mathbf{x}) = \int_G g(\mathbf{x},\mathbf{y})\eta(d\mathbf{y}) - \int_{\partial G}\left[u(\mathbf{z})\frac{\partial g(\mathbf{x},\mathbf{z})}{\partial \nu} - \frac{\partial u(\mathbf{z})}{\partial \nu}g(\mathbf{x},\mathbf{z})\right]d\mathbf{z} \qquad (13)$$

where Green's function

$$g(\mathbf{x},\mathbf{y}) = g^*(\|\mathbf{x}-\mathbf{y}\|) + \upsilon(\mathbf{x},\mathbf{y}), \qquad (14)$$

and $g^*(\|\mathbf{x}-\mathbf{y}\|)$ is the fundamental solution for the differential operator L, and

$$L\upsilon(\mathbf{x},\mathbf{y}) = 0, \qquad \mathbf{x}\in G,$$
$$\upsilon(\mathbf{x},\mathbf{y}) = -g^*(\|\mathbf{x}-\mathbf{y}\|), \qquad \mathbf{x}\in \partial G.$$

In order to generate realizations of a random field specified by such an SPDE we have to solve a boundary value problem in the given domain. For this reason we investigate the effect of the boundary on the random field and its covariance function. From (13) we note that homogeneous Dirichlet or Neumann boundary conditions allow one to construct a zero mean Gaussian random field with the covariance function

$$C(\mathbf{x},\mathbf{y}) = \int_G g(\mathbf{x},\mathbf{x_0})g(\mathbf{y},\mathbf{x_0})d\mathbf{x_0}. \qquad (15)$$

In contrast with equation (9) for the infinite domain, the covariance function can be non-stationary even for the Helmholtz equation when the domain is finite.

If the correlation distance is significantly shorter than the diameter of the domain G, which for the Helmholtz equation (12) means that,

$$d_{corr}(a) = \int_0^{+\infty}\rho_a(r)dr << \mathrm{diam}G, \qquad (16)$$

we can still assume that the correlation function (15) has approximately the same value as in the infinite domain case specified by equation (9). This

is valid only when points are taken away from the boundary. In order to estimate the difference between (15) and (9) near the boundary (which we will call "the distortion of the correlation function") we consider a half space domain $\mathbf{x} \in \mathbf{R}^3, \quad 0 \leq x < \infty$ with a

1. *Dirichlet boundary condition* $u(\mathbf{x}) = 0$ at $x = 0$

Green's function is:

$$g(x, y, z, \xi, \eta, \zeta) = g^*(x - \xi, y - \eta, z - \zeta) - g^*(x + \xi, y - \eta, z - \zeta)$$

where $g^*(x - \xi, y - \eta, z - \zeta)$ is the fundamental solution of (2); and with a

2. *Neumann boundary condition* $\partial_x u(\mathbf{x}) = 0$ at $x = 0$

Green's function is:

$$g(x, y, z, \xi, \eta, \zeta) = g^*(x - \xi, y - \eta, z - \zeta) + g^*(x + \xi, y - \eta, z - \zeta)$$

In general the covariance between two points (x, y, z) and $(x + \Delta x, y, z)$ is

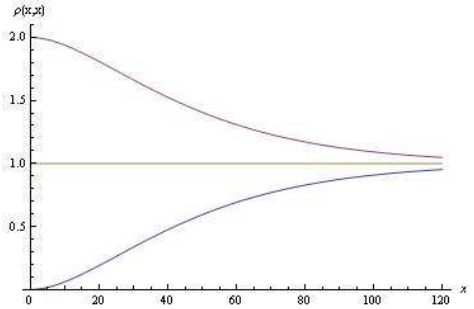
$$C(x, y, z, x + \Delta x, y, z) = \int_0^{+\infty} \int_{-\infty}^{+\infty} \int_{-\infty}^{+\infty} g(x, y, z, \xi, \eta, \zeta) g(x + \Delta x, y, z, \xi, \eta, \zeta) d\xi d\eta d\zeta.$$

With the Dirichlet boundary condition the covariance function is

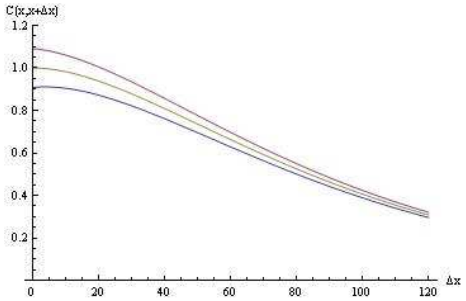
$$\begin{aligned} C(x, y, z, x + \Delta x, y, z) = \\ \int_0^{+\infty} \int_{-\infty}^{+\infty} \int_{-\infty}^{+\infty} g^*(x, y, z, \xi, \eta, \zeta) g^*(x + \Delta x, y, z, \xi, \eta, \zeta) - \\ g^*(x, y, z, -\xi, \eta, \zeta) g^*(x + \Delta x, y, z, \xi, \eta, \zeta) - \\ g^*(x, y, z, \xi, \eta, \zeta) g^*(x + \Delta x, y, z, -\xi, \eta, \zeta) + \\ g^*(x, y, z, -\xi, \eta, \zeta) g^*(x + \Delta x, y, z, -\xi, \eta, \zeta) d\xi d\eta d\zeta = \\ \int_{-\infty}^{+\infty} \int_{-\infty}^{+\infty} \int_{-\infty}^{+\infty} g^*(x, y, z, \xi, \eta, \zeta) g^*(x + \Delta x, y, z, \xi, \eta, \zeta) d\xi d\eta d\zeta - \\ \int_0^{+\infty} \int_{-\infty}^{+\infty} \int_{-\infty}^{+\infty} g^*(x, y, z, -\xi, \eta, \zeta) g^*(x + \Delta x, y, z, \xi, \eta, \zeta) + \\ g^*(x, y, z, \xi, \eta, \zeta) g^*(x + \Delta x, y, z, -\xi, \eta, \zeta) d\xi d\eta d\zeta \end{aligned}$$

The first integral is the non-distorted covariance (9), whereas the second integral represents the distortion of the covariance function near the plane at $x = 0$. For the Neumann boundary condition the distortion has the same magnitude but the opposite sign. If we are interested in determining the distortion in the variance only, $(\Delta x = 0)$, then the second integral reduces to,

$$\int_{-\infty}^{+\infty} \int_{-\infty}^{+\infty} \int_{-\infty}^{+\infty} g^*(x, y, z, \xi, \eta, \zeta) g^*(x, y, z, -\xi, \eta, \zeta) d\xi d\eta d\zeta.$$



(a) Variance $\sigma^2(x) = \rho(x, x)$ as a function of a distance from the boundary



(b) Covariance function at the distance $x = d_{corr}(a) = 100$ from the boundary

Figure 2: Neumann b.c., fundamental solution, Dirichlet b.c. Correlation distance $d_{corr}(a) = 2/a = 100$

In the one-dimensional case for Helmholtz equation, these integrals can be determined analytically:

$$C(x, y, z, x + \Delta x, y, z) = \frac{(1 + a\Delta x)e^{-a\Delta x}}{4a^3b^2} - \frac{e^{-a(2x+\Delta x)}(1 + a(2x + \Delta x))}{4a^3b^2}.$$

Choosing the parameter $b^2 = \frac{1}{4a^3}$ so as to normalize the covariance we obtain,

$$C(x, y, z, x + \Delta x, y, z) = (1 + a\Delta x)e^{-a\Delta x} - e^{-a(2x+\Delta x)}(1 + a(2x + \Delta x)).$$

For $x = d_{corr}(a) = 2/a$, the distortion in variance does not depend on a and is approximately 10% (see fig. 2).

A similar analysis can be done for the three-dimensional case where the integrals can be calculated numerically and for $x = d_{corr}(a) = 1/a$ the distortion in variance is approximately 13%. At points near edges and corners the distortion is larger and also can be estimated in a similar way.

We conclude from this analysis that the random field generated by the SPDE is significantly distorted if the distance from the boundary is shorter that correlation distance. As we discuss in the introduction to this section, the distortion provides a clear reason for being careful in choosing appropriate boundary conditions and not just using the natural conditions associated with the underlying deterministic PDE. Such a choice must depend on the application in mind, but in general we would propose that in two dimensions a stochastic ordinary differential equation be solved along the edges, and in three dimensions an SPDE be solved on the bounding surface after first solving an ordinary stochastic equation on the edges. The values at the corners could be simply sampled from a normal density with the appropriate mean and variance.

4 Numerical approximation of White Noise

In [1] the approximation of Gaussian white noise on rectangular grids was presented. We extend this approach to arbitrary grids. On a domain $G \subseteq \mathbf{R}^d$ with partition $\Gamma_h = \bigcup_{i=1}^N K_i$ into N cells, we approximate white noise as a piecewise constant function

$$\dot{\eta}_h(\mathbf{x}) = \sum_{K_i \in \Gamma_h} \frac{\chi_i(\mathbf{x})}{\mu(K_i)} \int_{K_i} \eta(d\mathbf{x}) = \sum_{K_i \in \Gamma_h} \frac{\eta_i}{\sqrt{\mu(K_i)}} \chi_i(\mathbf{x}) \tag{17}$$

where $\mu(K_i)$ is the volume of element K_i, $\chi_i(\mathbf{x})$ is the characteristic function for K_i and $\eta_i \sim N(0,1)$.

Lemma 4.1. *For modified white noise $\dot{\eta}_h(\mathbf{x}) \in L_2(G)$*

$$E(\int_G \dot{\eta}_h(\mathbf{x}) d\mathbf{x})^2 = \mu(G)$$

$$E(\|\dot{\eta}_h\|_{L_2}^2) = N$$

Proof.

$$E\left(\int_G \dot{\eta}_h d\mathbf{x}\right)^2 = E\left(\int_G \sum_{K_i \in \Gamma_h} \frac{\eta_i}{\sqrt{\mu(K_i)}} \chi_i(\mathbf{x}) d\mathbf{x}\right)^2 = E\left(\sum_{K_i \in \Gamma_h} \frac{\eta_i}{\sqrt{\mu(K_i)}} \int_{K_i} d\mathbf{x}\right)^2$$

$$= E\left(\sum_{K_i \in \Gamma_h} \eta_i \sqrt{\mu(K_i)}\right)^2 = \sum_{K_i \in \Gamma_h} \mu(K_i) = \mu(G)$$

Similarly,

$$E\left(\int_G \left(\dot{\eta}_h(\mathbf{x})\right)^2 d\mathbf{x}\right) = E\left(\int_G \left(\sum_{K_i \in \Gamma_h} \frac{\eta_i}{\sqrt{\mu(K_i)}} \chi_i(\mathbf{x})\right)^2 d\mathbf{x}\right)$$

$$= E\left(\int_G \sum_{K_i \in \Gamma_h} \frac{\eta_i^2}{\mu(K_i)} \chi_i(\mathbf{x}) d\mathbf{x}\right) = \sum_{K_i \in \Gamma_h} \int_G \frac{1}{\mu(K_i)} \chi_i(\mathbf{x}) d\mathbf{x} = \sum_{K_i \in \Gamma_h} 1 = N$$

□

The approximate elliptic stochastic equation

$$-\nabla^2 u_h(\mathbf{x}) + a^2 u_h(\mathbf{x}) = \dot{\eta}_h(\mathbf{x}), \quad \mathbf{x} \in G, \quad u_h|_{\partial G} = 0 \tag{18}$$

possesses the unique solution

$$u_h(\mathbf{x}) = \int_G g(\mathbf{x},\mathbf{y})\dot{\eta}_h(\mathbf{y})d\mathbf{y}. \tag{19}$$

Convergence of $u_h(\mathbf{x})$ to $u(\mathbf{x})$ was shown in [1] for the one-dimensional case based on the Lipschitz property of Green's function and in [20] it was extended to the 2- and 3-dimensional cases for rectangular grids. In both papers a constraint was imposed on parameter a in equation (18) (see Theorem 2.1 in [20]). In this work we eliminate this constraint and extend the proof for arbitrary grids.

Theorem 4.1. *Suppose that u and u_h are the exact and approximate solutions respectively, then for $0 < \varepsilon < 1/4$*

$$E(\|u-u_h\|_{L^2}^2) \le Ch^{1-\varepsilon} \quad for\ d=2, \tag{20}$$

$$E(\|u-u_h\|_{L^2}^2) \le Ch^{\frac{3}{4}-\varepsilon} \quad for\ d=3. \tag{21}$$

Proof. Let $e(x) = u(x) - u_h(x) = \int_G g(x,y)\eta(dy) - \int_G g(x,y)\dot{\eta}_h(y)dy$.

$$\begin{aligned} E[e^2(x)] &= E[(\sum_{K_i\in\Gamma_h}\int_{K_i}(g(x,y) - \frac{1}{\mu(K_i)}\int_{K_i} g(x,z)dz)\eta(dy))^2] = \\ &= \frac{1}{\mu(K_i)^2}\sum_{K_i\in\Gamma_h}\int_{K_i}(\int_{K_i} g(x,y) - g(x,z)dz)^2dy \\ &\le \frac{1}{\mu(K_i)}\sum_{K_i\in\Gamma_h}\int_{K_i^2}|g(x,y)-g(x,z)|^2\,dzdy \end{aligned}$$

$$E(\|u-u_h\|_{L^2}^2) = \int_G E(e^2(x))dx \le$$

$$\frac{1}{\mu(K_i)}\sum_{K_i\in\Gamma_h}\int_{K_i^2}(\int_G |g(x,y)-g(x,z)|^2\,dx)dzdy$$

For Helmholtz equation (18) Green's function for $d=3$ is

$$g(x,y) = \frac{e^{-a|x-y|}}{|x-y|} + \upsilon(x,y),$$

where $\upsilon(x,y)$ is a harmonic, Lipschitz continuous function on G that depends on the shape of G. From Lemma A.2 we obtain

$$\int_G |g(x,y)-g(x,z)|^2\,dx \le c_\varepsilon\,|y-z|^{\frac{3}{4}-\varepsilon}$$

Hence

$$E(\|u-u_h\|_{L^2}^2) \leq \frac{c_\varepsilon}{\mu(K_i)} \sum_{K_i \in \Gamma_h} \int_{K_i^2} |y-z|^{\frac{3}{4}-\varepsilon} \, dzdy \leq$$

$$\frac{c_\varepsilon}{\mu(K_i)} \sum_{K_i \in \Gamma_h} \int_{K_i^2} h^{\frac{3}{4}-\varepsilon} dzdy = c_\varepsilon \sum_{K_i \in \Gamma_h} \int_{K_i} h^{\frac{3}{4}-\varepsilon} dy = Ch^{\frac{3}{4}-\varepsilon}.$$

For $d = 2$ Green's function is $g(x,y) = K_0(a\,|x-y|) + \upsilon(x,y)$. Analogously to the 3-D case we apply Lemma A.2 and obtain (20). □

5 A Stochastic sampling algorithm in parametric and physical space.

5.1 Sampling in parametric space

To generate realizations of a Gaussian stationary random field, we state a boundary value problem for Helmholtz equation (12) driven by approximate Gaussian 'white noise' (17) with homogeneous Neumann boundary conditions. This problem is solved numerically in the two-dimensional case using a Finite Element method on the triangulated region. Field realizations for the same realization of white noise and for various values of the coefficient a are shown on figure 3. To obtain anisotropic correlation functions in 2-D (see fig. 4), $\rho(r) = arK_1(ar)$ with $r = \sqrt{\alpha^2 x^2 + \beta^2 y^2}$ one can use the equation

$$-\frac{1}{\alpha^2}\xi''_{xx}(x,y) - \frac{1}{\beta^2}\xi''_{yy}(x,y) + a^2\xi(x,y) = \dot{\eta}(x,y). \tag{22}$$

5.2 Sampling in physical space

Our goal is to model a field which is "locally stationary", that is, at each point $\mathbf{x}$ there is a local orthonormal basis $\mathbf{h}_i(\mathbf{x})$, $i = 1...d$ where the field can be considered as stationary in the small neighborhood of the point $\mathbf{x}$ with correlation function $C(\sqrt{\sum_i \alpha_i^2 x_i^2})$, where coefficients α_i, $i = 1...d$ are constant within this neighborhood and represent anisotropy of the correlation function. The shape of the geological layer provides sufficient information to find these base vectors on the boundary of the layer and we reconstruct vector components inside the layer via boundary value problems for Laplace's equation (Fig. 5).

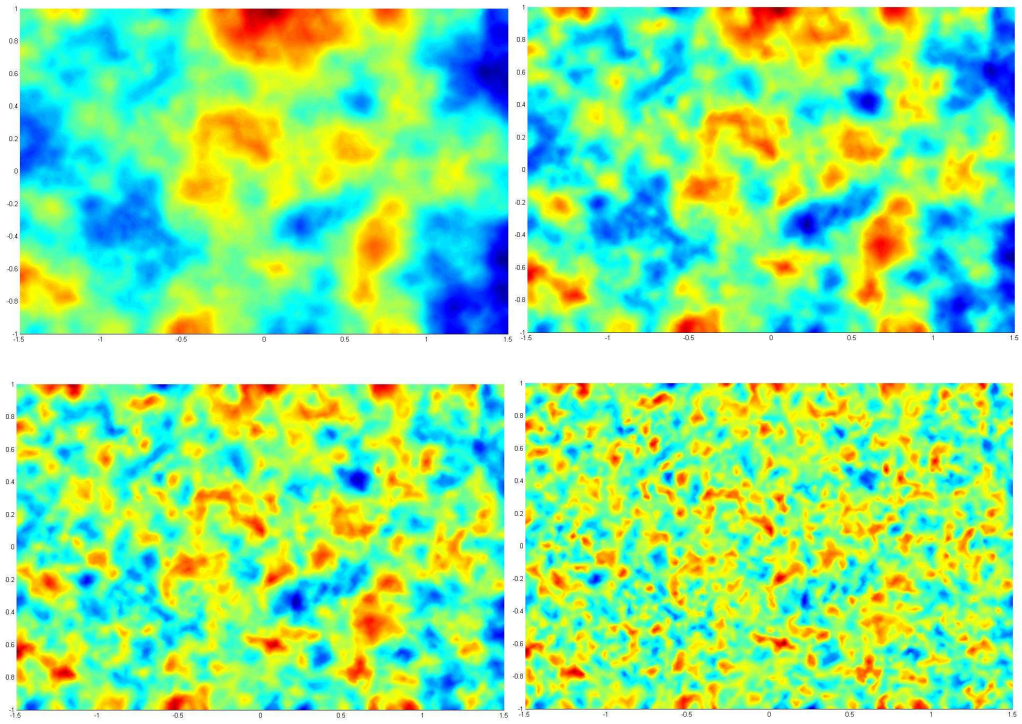


Figure 3: Field realizations for Helmholtz equation (12): a=5, 10, 20, 50. Correlation function $\rho(r) = ar \cdot K_1(ar)$.

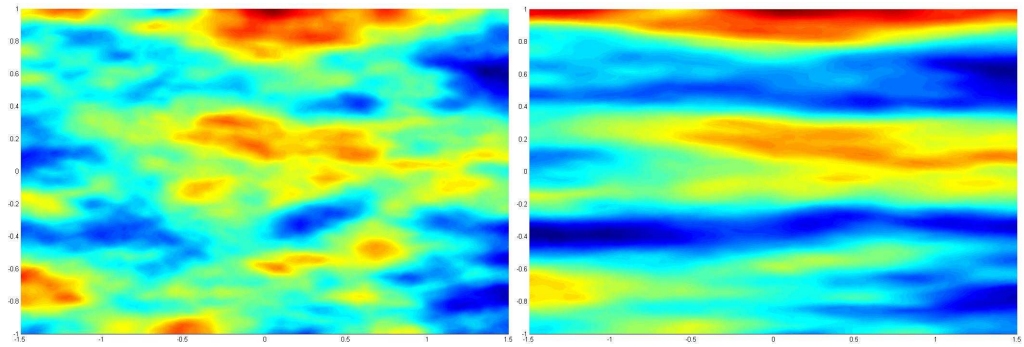


Figure 4: Field realizations for equation (22): $a = 10$, $\alpha = 0.32$, $\beta = 1$ (left), $a = 10$, $\alpha = 0.1$, $\beta = 1$ (right).

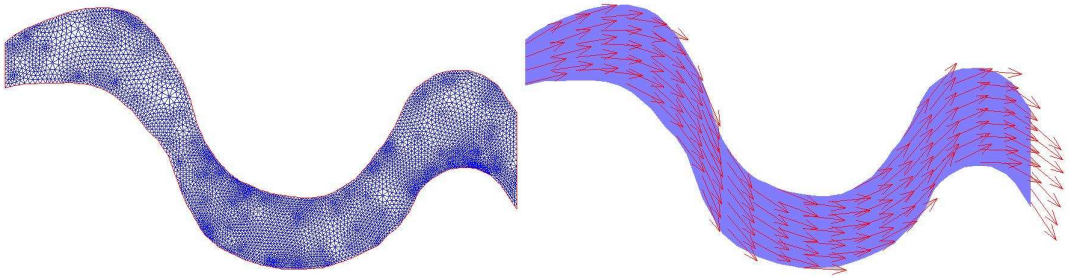


Figure 5: A triangulated geological layer and the $\mathbf{h}_1(\mathbf{x})$ vector field.

In order to generate samples in physical space, that is, directly on curved geological layers, we introduce the equation

$$-\nabla \cdot \mathbf{A}(\mathbf{x})\nabla\xi(\mathbf{x}) + a^2\xi(\mathbf{x}) = \dot{\eta}(\mathbf{x}) \tag{23}$$

where $\mathbf{A}$ is a second order symmetric tensor which has a diagonal matrix representation A_{ij} in the basis $\mathbf{h}_i(\mathbf{x})$, $i = 1...d$ with diagonal components α_i^{-2}, $i = 1...d$, i.e. using the symbol $\otimes$ to denote the dyadic product

$$\mathbf{A} = \frac{1}{\alpha_1^2}\mathbf{h}_1 \otimes \mathbf{h}_1 + \frac{1}{\alpha_2^2}\mathbf{h}_2 \otimes \mathbf{h}_2 + \frac{1}{\alpha_3^2}\mathbf{h}_3 \otimes \mathbf{h}_3.$$

Hence equation (23) in the global coordinates becomes

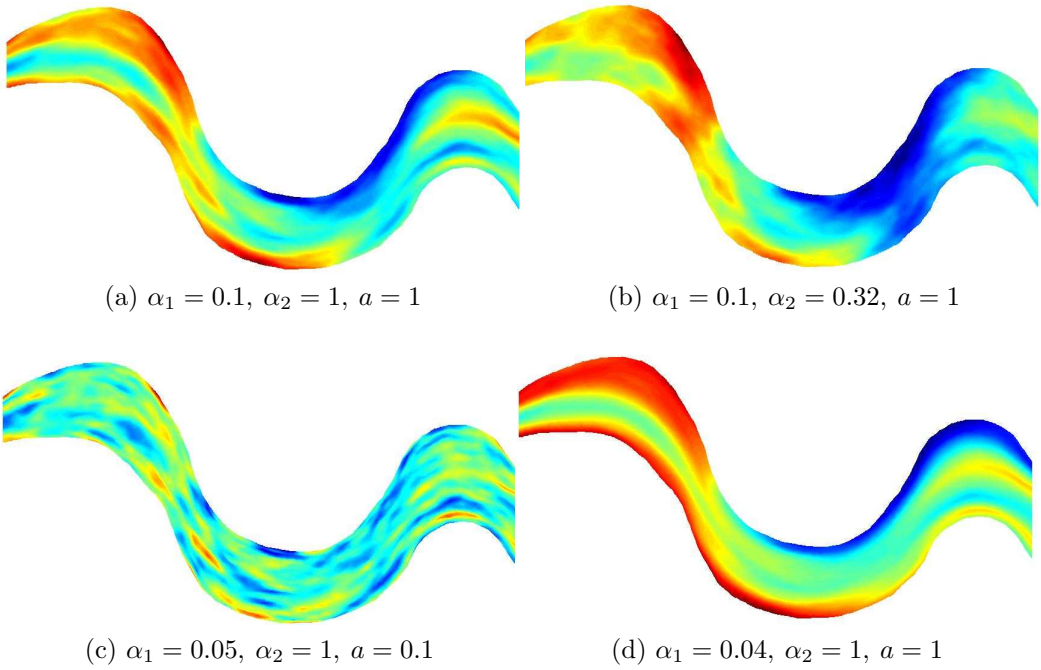
$$-\nabla \cdot L(\mathbf{x})AL^T(\mathbf{x})\nabla\xi(\mathbf{x}) + a^2\xi(\mathbf{x}) = \dot{\eta}(\mathbf{x}), \tag{24}$$

where $\mathbf{h}_i$ are columns in the matrix L and A is the constant diagonal matrix of correlation anisotropy coefficients α_i^{-2}. This equation can be used in the global coordinates even when it is impossible to construct layer-following stratigraphic coordinates.

Fields of reservoir characteristics, such as porosity and permeability, usually have longer correlation distances along a curved layer in comparison with the correlation distances across the layer. Samples generated from equation (24) shown in fig. 6 demonstrate this anisotropy.

5.3 Markov property of a discretized random field.

In section 2.2 we mentioned the Markov property of the continuous random field (5). This property is preserved for discrete random fields obtained as Finite Element approximations of (5). Indeed, for each grid node i and its



(a) $\alpha_1 = 0.1,\ \alpha_2 = 1,\ a = 1$ (b) $\alpha_1 = 0.1,\ \alpha_2 = 0.32,\ a = 1$

(c) $\alpha_1 = 0.05,\ \alpha_2 = 1,\ a = 0.1$ (d) $\alpha_1 = 0.04,\ \alpha_2 = 1,\ a = 1$

Figure 6: Field realizations for the equation (24).

neighborhood $\mathcal{N}_i$ of nodes sharing an edge with the node i, the numerical scheme produces the equations

$$a_i\xi_i + \sum_{j\in\mathcal{N}_i} a_j\xi_j = \eta_i \qquad \eta_i \sim N(0,\sigma) \tag{25}$$

which is equivalent to the definition of a discrete Gaussian Markov random field.

Two distant points i and j are connected by a graph of local relations (25) but in our approach we do not use the correlation distance and therefore the stratigraphic distance between them. This advantage enables the method to provide the Markov property in the field that is generated and with the advantage that the scaling from the metric structure of the geological system is automatically accounted for by the partial differential equation.

5.4 Geological faults and a modified Finite Volume method.

Geological faults play a significant role in description and modeling of hydrocarbon reservoirs, therefore we propose a strategy for sampling in physical

space in the presence of faults. Consider a fault surface S which can split a layer into subregions or introduce a localized displacement of rocks (as on fig. 8) and the mapping between two sides of the fault surface $\mathbf{f}(\mathbf{x}) : S \to S$ (fig. 7).

For modelling discontinuities across a fault in 3-D we propose the following modification of the Finite Volume method. The integral form of equation (24) is discretized for each control volume ω_i (grid cell) as follows:

$$\sum_{\sigma \in \partial\omega_i} F_{i,\sigma} + a^2 \mu(\omega_i) \cdot u_i = \int_{\omega_i} \eta(d\mathbf{x})$$

where $\mu(\omega_i)$ is the volume of ω_i and $F_{i,\sigma}$ is the approximated flux across the face $\sigma \in \partial\omega_i \cap \partial\omega_j$ shared by the volume ω_i and one of its neighboring volumes ω_j. That is, the analytical flux

$$F_{i,\sigma} = \int_{\sigma} -A(\mathbf{x}) \nabla u \cdot \mathbf{n} ds$$

is approximated by $F_{i,\sigma} = -T_{ij}(u_j - u_i)$, where $A(\mathbf{x})$ is the tensor from the equation (23) and the coefficient T_{ij} depends on the area of the face σ and the tensor $A(\mathbf{x})$ averaged over the respective grid cells ω_i and ω_j.

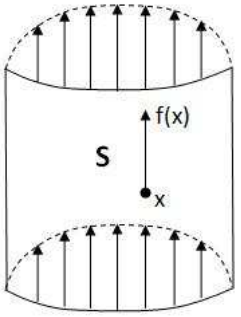


Figure 7: Fault surface S and displacement $\mathbf{f}(\mathbf{x})$.

In the modified Finite Volume method we exclude all fluxes across faces which belong to a fault surface and add fluxes between pairs of volumes which shared a face before the layer was faulted. That is, for control volumes ω_i, ω_j with faces $\sigma_1 \in \partial\omega_i \cap S, \sigma_2 \in \partial\omega_j \cap S$ if the intersection $\sigma_1 \cap \mathbf{f}(\sigma_2)$ is not empty we add the flux $-T_{ij}(u_j - u_i)$ to the equations for the volume ω_i and the same flux with the opposite sign to the equation for the volume ω_j. The coefficient T depends on the area of intersection $\sigma_1 \cap \mathbf{f}(\sigma_2)$, although this area does not exist in the grid geometry of the model.

We apply this method to generate fields of basis vectors and random fields. Figure 8 shows the application of the described method and a generated realization of a random field with an exponential anisotropic correlation function.

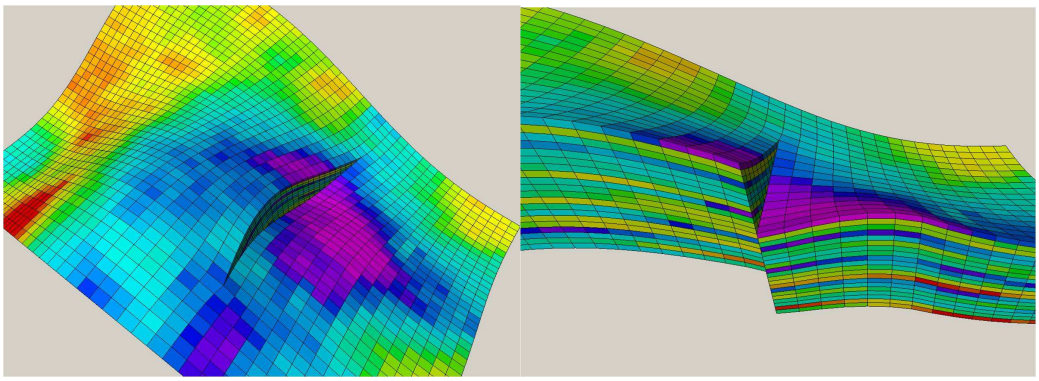


Figure 8: 3D case: Field realizations for the equation (24) in the presence of a localised geological fault.

6 Relation to Tikhonov regularization. Conditional sampling.

6.1 SPDE priors as functional measures

Consider a random field $\xi(\mathbf{x})$ with zero mean and a functional probability density of the form

$$\pi(\xi) = \frac{1}{Z}\exp(-H[\xi]) \tag{26}$$

where

$$H[\xi] = \frac{1}{2}\int_G [a_2(\nabla^2\xi)^2 + a_1(\nabla\xi)^2 + a_0\xi^2]d\mathbf{x}, \tag{27}$$

and Z is a normalization constant such that

$$\int_S \pi(\xi)D[\xi] = 1$$

where $D[\xi]$ denotes integration over some suitable space of functions (see Appendix L in [3] for details on functional differentiation and integration). Using Gauss' theorem and assuming suitable vanishing boundary conditions this can be written in the form

$$H[\xi] = \frac{1}{2}\int_G \xi L\xi d\mathbf{x},$$

where $L\xi$ is

$$L\xi = a_2\nabla^2(\nabla^2\xi) - a_1(\nabla^2\xi) + a_0\xi$$

It can be shown (see [10] for details) that Green's function $g(\mathbf{x}, \mathbf{y})$ defined as a solution of the equation

$$Lg(\mathbf{x}, \mathbf{y}) = \delta(\mathbf{x} - \mathbf{y})$$

is the covariance function of the field $\xi(\mathbf{x})$, i.e.

$$E[\xi(\mathbf{x})\xi(\mathbf{y})] = g(\mathbf{x}, \mathbf{y}).$$

Therefore from (10) we deduce that for the solution of Helmholtz equation $-b\nabla^2\xi(\mathbf{x}) + ba^2\xi(\mathbf{x}) = \dot{\eta}(\mathbf{x})$ the functional probability density has the form (26) with functional

$$H[\xi] = \frac{1}{2}\int_G [b^2(\nabla^2\xi)^2 + 2b^2a^2(\nabla\xi)^2 + b^2a^4\xi^2]d\mathbf{x}.$$

The example of the stochastic modified Helmholtz equation does not lead to correlation functions with oscillatory features. This can be achieved by adding bi-harmonic terms to the SPDE, as we will indicate later. When this is done, the equivalent functional measure involves fourth order derivatives. As one can sample from such measures using the stochastic partial differential Langevin equation we have the interesting result that sampling from a functional measure, with a parabolic equation is equivalent to sampling using an elliptic problem, where the spatial differential operator is a 'square-root' of the spatial part of the operator in the Langevin equation. This is the reason for the potential increased efficiency in sampling by using a stochastic elliptic PDE. However, the main interest in this is not to do with efficiency (as the time spent to initialize an ensemble is generally negligible when compared to the time spent in the subsequent solution of the forward problem). In practice the main interest arises from the lower order of the spatial operator, making it much easier to construct numerical approximations to the equations.

6.2 Bayesian formulation of inverse problems.

The following idea is applicable to an inverse problem, including time dependent problems, in abstract generality (as in [9]). However, here we will just use a simple example for the purpose of linking the SPDE approach to the classical Tikhonov regularisation methods. Consider the problem of diffusion in a heterogeneous medium with diffusion coefficient $k(\mathbf{x})$ such that $k = \ln(\xi(\mathbf{x}))$. The equation for the solution will be

$$-\nabla \cdot k(\mathbf{x})\nabla p(\mathbf{x}) = 0, \quad \mathbf{x} \in G. \tag{28}$$

The inverse problem requires determination or at least a characterization of both functions $k(\mathbf{x})$ and $p(\mathbf{x})$ when their values, or some function of the values are only known at a few points, generally with some measurement error. These observations can be written as a diagnostic functional $\alpha = D[\xi(\mathbf{x}), p(\mathbf{x})]$. However, the equation (28) defines the solution as a functional of the coefficient k and the boundary data which we assume to be known. This can be written as $\alpha = A[\xi(\mathbf{x})]$.

The Bayesian formulation of the inverse problem is given by the equation

$$\pi(\xi|\alpha^*) = \frac{\delta_\sigma(\alpha^* - A[\xi])\pi(\xi)}{\int_S \delta_\sigma(\alpha^* - A[\xi])\pi(\xi)D[\xi]}$$

where α^* are the actual values of the measurements and δ_σ stands for a product of small-variance Gaussian functionals over the different measurements.

Now consider the case where the prior distribution is of the form (26). If the field of properties ξ is computed so that it maximizes the probability density functional then this is equivalent to minimizing the functional

$$H^*[\xi] = \sum_i \frac{(\alpha_i^* - A_i[\xi])^2}{2\sigma_i^2} + H[\xi]$$

where $H[\xi]$ is defined by (27) and the subscript i ranges over a finite number of different measurements.

Using the notation of equation (27) for various choices of a_0, a_1 and a_2 a variety of well known regularisation procedures are derived. In particular the choices $a_0 > 0, a_1 = 0, a_2 = 0$ corresponds to 'Tikhonov order-0', $a_0 = 0, a_1 > 0, a_2 = 0$ corresponds to 'Tikhonov order-1' and $a_0 = 0, a_1 = 0, a_2 > 0$ corresponds to 'Tikhonov order-2' regularisation [18].

It thus becomes clear that the classical Tikhonov regularisation methods are equivalent to maximum probability Bayesian inversion with a Gaussian prior. When this idea is extended to the application of SPDE priors, such as the Helmholtz equation, we see that we cannot in general show equivalence with the 'pure' Tikhonov regularisations of various orders but with a 'mixed' version that includes more than one order of regularisation. While one might regard this loss of generality as a disadvantage, one might remark that the 'pure' methods, when examined from a Bayesian point of view, do not usually give rise to correlation functions that are typical of the textures of the functions that are modelled by the associated stochastic process.

6.3 Conditional stochastic simulation.

Suppose that the function is known at a few points $\xi(\mathbf{x}_k) = \xi_k^*$ and we want to generate only those realizations of the random field which are consistent

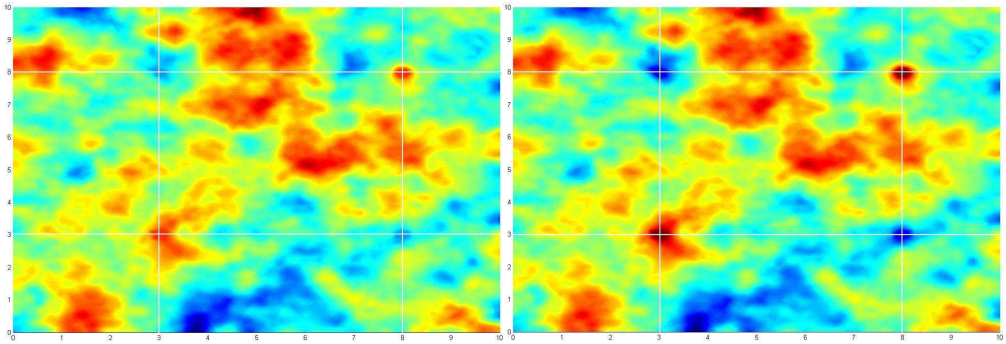


Figure 9: Solutions of (29) which are consistent with observations (marked by line intersections): $\xi(3,3) = -\xi(3,8) = \xi(8,8) = -\xi(8,3) = 0.3$ and 0.5 accordingly.

with the observations. This procedure is called 'conditional simulation' in the geostatistics literature and can also be defined via stochastic PDEs as follows.

To motivate the equation that is used, we formulate a formal minimization problem for the functional

$$H[\xi] = \frac{1}{2}\int_G [b(\nabla\xi)^2 + ba^2\left(\xi - \frac{\dot{\eta}_h}{ba^2}\right)^2]d\mathbf{x}$$

subject to constraints $\xi(\mathbf{x}_k) = \xi_k^*$ and $\frac{\partial\xi}{\partial n} = 0$ on ∂G.

Introducing Lagrange multipliers this can be rewritten as

$$\hat{H}[\xi] = \frac{1}{2}\int_G [b(\nabla\xi)^2 + ba^2\left(\xi - \frac{\dot{\eta}_h}{ba^2}\right)^2]d\mathbf{x} + \sum_k \gamma_k(\xi(\mathbf{x_k}) - \xi_k^*).$$

Taking functional derivatives with respect to ξ and partial derivatives with respect to the γ_k, we obtain a system

$$-b\nabla^2\xi(\mathbf{x}) + ba^2\xi(\mathbf{x}) = \sum_k \gamma_k\sigma(\mathbf{x} - \mathbf{x}_k) + \dot{\eta}_h(\mathbf{x}) \quad (29)$$

$$\xi(\mathbf{x_k}) = \xi_k^* \quad (30)$$

with boundary condition $\frac{\partial\xi}{\partial n} = 0$ on ∂G. It follows from theorem 4.1 that $\xi(\mathbf{x})$ converges to the solution of the equation (29) with $\dot{\eta}(\mathbf{x})$ when h goes to zero. Figure 9 shows numerical solutions for this system of equations with the same realization of the approximate white noise and two different sets of observations.

7 Biharmonic-Helmholtz equation.

7.1 Oscillatory correlation functions.

In this section we consider properties of the Biharmonic-Helmholtz equation (noting once again that the full name would refer to the modified Helmholtz equation):

$$a\nabla^2(\nabla^2 u) + b\nabla^2 u + cu = \dot{\eta}(\mathbf{x}) \tag{31}$$

Using Fourier transforms one can show that Green's function in 2-D is given by

$$G(r) = \frac{1}{(2\pi)^2}\int_{-\infty}^{\infty}\int_{-\infty}^{\infty}\frac{e^{i\mathbf{k}\cdot\mathbf{r}}}{ak^4 - bk^2 + c}dk_1 dk_2.$$

Using polar coordinates and noticing that $\int_0^{2\pi} e^{i\rho r\cos\theta}d\theta = 2\pi J_0(\rho r)$ this integral reduces to

$$G(r) = \frac{1}{2\pi}\int_0^{\infty}\frac{\rho J_0(\rho r)}{a\rho^4 - b\rho^2 + c}d\rho.$$

where J_0 is the Bessel function of the first kind. Using theorem 2.1 we obtain the covariance function

$$C(r) = \frac{1}{2\pi}\int_0^{\infty}\frac{\rho J_0(\rho r)}{(a\rho^4 - b\rho^2 + c)^2}d\rho. \tag{32}$$

In general this correlation function is a decaying and oscillatory function. There are values of the parameters that give a simple decay. In 1-D and 3-D Green's and correlation functions have the same qualitative form as in 2-D (see [10] for details).

In order to solve the Biharmonic-Helmholtz equation numerically, we represent it as a system of two second order elliptic equations with homogeneous Neumann boundary conditions.

$$\begin{aligned} a\nabla^2 v + bv + cu &= \dot{\eta}(\mathbf{x}), \\ -\nabla^2 u + v &= 0. \end{aligned}$$

An example of the correlation function (32) obtained via numerical integration and a random field sample generated with the same parameters $a = 1, b = 4.47, c = 21.37$ are shown on figure 10.

7.2 Gaussian correlation function.

The correlation function of the form of a Gaussian density is widely used in geostatistics, and the Biharmonic-Helmholtz equation can be used to generate samples with a correlation function close to a Gaussian correlation. As

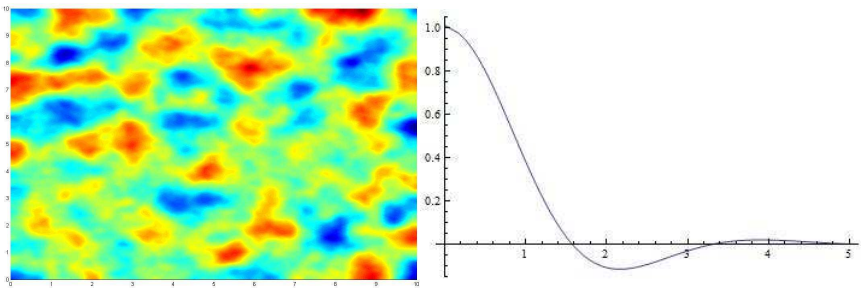


Figure 10: A sample of the random field for equation (31) with oscillatory correlation function.

before we consider a white noise driven equation

$$Lu(\mathbf{x}) = \dot{\eta}(\mathbf{x}), \quad \mathbf{x} \in \mathbf{R}^d \quad d = 1, 2, 3$$

and we are looking for the linear differential operator in the form

$$L = \sum_{n=0}^{\infty} a_n (\nabla^2)^n$$

which provides a solution with the correlation function

$$C(r) = e^{-\frac{r^2}{\lambda^2}} \tag{33}$$

It was shown in section 2.2 that the correlation function $C(r)$ satisfies the equation

$$L^2 C(r) = \delta(r).$$

We consider the two-dimensional case here noting that the 1- and 3-D cases are proved analogously. Applying a Fourier transform we obtain the algebraic equation

$$\hat{L}^2(\omega_x, \omega_y)\hat{C}(\omega_x, \omega_y) = \frac{1}{2\pi}$$

The transform of a Gaussian correlation is

$$\hat{C}(\omega_x, \omega_y) = \frac{\lambda^2}{2\pi} e^{-\frac{\lambda^2(\omega_x^2+\omega_y^2)}{4}},$$

and hence,

$$\begin{aligned}
\hat{L}(\omega_x, \omega_y) &= \frac{1}{\lambda} e^{\frac{\lambda^2(\omega_x^2+\omega_y^2)}{8}} \\
&= \frac{1}{\lambda} \sum_{n=0}^{\infty} \left(\frac{\lambda^2}{8}\right)^n \frac{1}{n!} (\omega_x^2 + \omega_y^2)^n \\
&= \frac{1}{\lambda} \sum_{n=0}^{\infty} \left(-\frac{\lambda^2}{8}\right)^n \frac{1}{n!} ((i\omega_x)^2 + (i\omega_y)^2)^n.
\end{aligned}$$

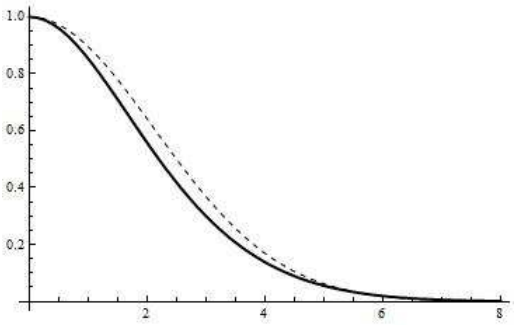


Figure 11: Correlation functions ($\lambda = 3$): Gaussian function (dashed line), function (32) for the equation (34).

Taking the inverse Fourier transform leads to the result,

$$\begin{aligned} L &= \frac{1}{2\pi\lambda}\sum_{n=0}^{\infty}\left(-\frac{\lambda^2}{8}\right)^n\frac{1}{n!}(\nabla^2)^n \\ &= \frac{1}{2\pi\lambda}e^{-\frac{\lambda^2}{8}\nabla^2}. \end{aligned}$$

Truncating terms for $n \geq 3$ we obtain the Biharmonic-Helmholtz equation, for which the correlation function (32) represents an approximation to (33) (see fig. 11).

$$\frac{1}{2\pi\lambda}(\frac{\lambda^4}{128}\nabla^2(\nabla^2 u) - \frac{\lambda^2}{8}\nabla^2 u + u) = \dot{\eta}(\mathbf{x}) \tag{34}$$

In this way we are able to approximate general non-local Gaussian random fields using a local approach. However this approach, as we hope we have demonstrated in the earlier sections, allows for the useful generalisation of the idea of a Gaussian random field in a geometry with complicated spatial features such as curved layers and faults.

8 Conclusions.

This paper has investigated the application of stochastic elliptic partial differential equations as priors for the solution of inverse problems. Of particular concern is the provision of a technique that can avoid the need to construct stratigraphic coordinates, which is generally very difficult or even impossible. We hope that the relatively simple idea that we have investigated solves this problem and stimulates further work. In particular further work on the implications of various lower dimensional models as boundary conditions is

required. Generalisations involving nonlinear terms and more complicated spatial variations in the tensor coefficients could be fruitful lines of research.

9 Acknowledgments.

We would like to thank Ben Hambly and David Allwright for their useful remarks and help. R.V. Potsepaev thanks Schlumberger for support and for permission to contribute to this paper. M. Aziz thanks the EPSRC and Schlumberger for their support.

This publication is based on work by C.L. Farmer, supported by Award Number KUK-C1-013-04, made by King Abdullah University of Science and Technology (KAUST).

Appendix.

The following statement was proved as part of Lemma 2.1. in [4]:

Lemma A.1. *For* $x, z \in G \subseteq \mathbf{R}^d, \quad d = 2, 3$ *and* $\varepsilon > 0$

$$\int_G \left|\log|x-y| - \log|z-y|\right|^2 dy \leq c_\varepsilon |x-z|^{1-\varepsilon};$$

for $0 < \varepsilon < 1/4$

$$\int_G \left|\frac{1}{|x-y|} - \frac{1}{|z-y|}\right|^2 dy \leq c_\varepsilon |x-z|^{\frac{3}{4}-\varepsilon}.$$

We also formulate the following

Lemma A.2. *For* $x, z \in G \subseteq \mathbf{R}^d, \quad d = 2, 3, \quad a > 0$ *and* $\varepsilon > 0$

$$\int_G |K_0(a|x-y|) + g(x,y) - K_0(a|z-y|) - g(z,y)|^2 dy \leq c_\varepsilon |x-z|^{1-\varepsilon}; \tag{35}$$

for $0 < \varepsilon < 1/4$

$$\int_G \left|\frac{e^{-a|x-y|}}{|x-y|} + g(x,y) - \frac{e^{-a|z-y|}}{|z-y|} - g(z,y)\right|^2 dy \leq c_\varepsilon |x-z|^{\frac{3}{4}-\varepsilon}. \tag{36}$$

where $g(x,y)$ *is Lipschitz continuous in* G *with respect to its first argument.*

Proof. The function $K_0(ax) - \log \frac{1}{x}$ is bounded and has bounded derivative on the segment $[0, d_G]$, where d_G is the diameter of the domain G. Therefore it is Lipschitz continuous on $[0, d_G]$, and

$$\left| K_0(a\,|x-y|) - \log \frac{1}{|x-y|} - K_0(a\,|z-y|) + \log \frac{1}{|z-y|} \right| \leq$$

$$C\,||x-y| - |z-y|| \leq C\,|x-z|$$

By definition there is $\Lambda > 0$ such that $|g(x,y) - g(z,y)| \leq \Lambda\,|x-z|$ for all x, y, z in G. Hence, by Lemma A.1 we have

$$\int_G |K_0(a\,|x-y|) + g(x,y) - K_0(a\,|z-y|) - g(z,y)|^2\,dy \leq$$

$$\int_G |\log|x-y| - \log|z-y| + (C+\Lambda)\,|x-z||^2\,dy \leq$$

$$c_\varepsilon^*\,|x-z|^{1-\varepsilon} + 2\sqrt{c_\varepsilon^*(C+\Lambda)}\,|x-z|^{\frac{3}{2}-\frac{\varepsilon}{2}} + (C+\Lambda)\,|x-z|^2 \leq$$

$$(c_\varepsilon^* + 2\sqrt{c_\varepsilon^*(C+\Lambda)}d_G^{\frac{1}{2}+\frac{\varepsilon}{2}} + (C+\Lambda)d_G^{1+\varepsilon})\,|x-z|^{1-\varepsilon} = c_\varepsilon\,|x-z|^{1-\varepsilon}.$$

For $d = 3$ noting that the function $\frac{e^{-ax}-1}{x}$ is bounded and has bounded derivative on the segment $[0, d_G]$ the proof is analogous to the 2-dimensional case. □

References

[1] Allen E., Novosel S., and Zhang Z. *Finite element and difference approximation of some linear stochastic partial differential equations.* Stochastics and Stochastics Rep., 64 (1998), 117-142.

[2] Baker R. *Modeling soil variability as a random field.* Math. Geology, 16: 435-448, 1984.

[3] Binney J.J., Dowrick N.J., Fisher A.J., Newman M.E.J. The Theory of Critical Phenomena. Oxford University Press, Oxford, 1992.

[4] Buckdahn R., Pardoux E. *Monotonicity methods for white noise driven quasi-linear PDEs.* In Pinsky M., eds. Diffusion Processes and Related Problems in Analysis, vol 1. Boston: Birkhauser, 1990, 219-233.

[5] Chilès J.-P., Delfiner P. Geostatistics: Modeling Spatial Uncertainty. John Wiley, New York, 1999.

[6] Christakos G. Random Field Models in Earth Sciences, Dover, 1992.

[7] Evensen G. Data Assimilation: The Ensemble Kalman Filter, Springer-Verlag,2007.

[8] Farmer C.L. *Local Geostatistics*, Paper A005 in the Proceedings of the 9th European Conference on Mathematics of Oil Recovery, Cannes, 2004.

[9] Farmer C.L. *Geological modelling and reservoir simulation* in: Mathematical Methods and Modeling in Hydrocarbon Exploration and Production, A. Iske, T. Randen (eds.), Springer-Verlag, Heidelberg, 119-212, 2005.

[10] Farmer C.L. *Bayesian field theory applied to scattered data interpolation and inverse problems* in: Algorithms for Approximation, A. Iske, J. Levesley (eds.), Springer-Verlag, Heidelberg, 147-166, 2007.

[11] Geman S., Geman D. *Stochastic relaxation, Gibbs distribution and the Bayesian restoration of images.* IEEE Transactions on Pattern Analysis and Machine Intelligence 6, 721-741, 1984.

[12] Heine V. *Models for two-dimensional stochastic process.* Biometrika, 42: 170-178, 1955.

[13] King P.R., Smith P.J. *Generation of correlated properties in heterogeneous porous media.* Math. Geology, 20: 863-877, 1988.

[14] Oksendal B. Stochastic Differential Equations - 6-th ed. Springer, 2007.

[15] Pitt L.D. *A Markov property for Gaussian processes with a multidimensional parameter.* Arch. Rat. Mech. Anal., 43, 367-391, 1971.

[16] Rozanov Ju.A. *Markov random fields and stochastic partial differential equations.* Mathematics of the USSR - Sbornik, v.35, n.1, 157-164, 1979.

[17] Rozanov Ju.A. Markov random fields, Springer-Verlag, New York, 1982.

[18] Tikhonov A.N., Arsenin V. Solution of Ill-posed Problems, Wiley, New York, 1977.

[19] Whittle P. *On stationary processes in the plane.* Biometrika, 41, 434-449, 1954.

[20] Yao R., Bo L. *Discontinuous Galerkin method for elliptic stochastic partial differential equations on two and three dimensional spaces.* Science in China Series A: Mathematics, 2007, vol. 50, No. 11, 1661-1672.

RECENT REPORTS

22/09	Tangent unit-vector fields: nonabelian homotopy invariants and the Dirichlet energy	Majumdar Robbins Zyskin
23/09	Morphological instability of a nonequilibrium icecolloid interface	Peppin Majumdar Wettlaufer
24/09	The effect of polar lipids on tear film dynamics	Aydemir Breward Witelski
25/09	Preconditioning for active set and projected gradient methods as semi-smooth Newton methods for PDE-constrained optimization with control constraints	Stoll Wathen
26/09	Functional differential equations arising in cell-growth	Wake Begg
27/09	A Cell Growth Model Revisited	Derfel van Brunt Wake
28/09	Quasi-steady state reduction of molecular motor-based models of directed intermittent search	Newby Bressloff
29/09	All-at-once preconditioning in PDE-constrained optimization	Rees Stoll Wathen
30/09	An hp-Local Discontinuous Galerkin method for Parabolic Integro-Differential Equations	Pani Yadav
31/09	Stochastic neural field theory and the system-size expansion	Bressloff
32/09	A Hamiltonian Krylov-Schur-type method based on the symplectic Lanczos process	Benner Faßbender Stoll
33/09	Nematic liquid crystals : from Maier-Saupe to a continuum theory	Ball Majumdar
34/09	Tangent unit-vector fields: nonabelian homotopy invariants and the Dirichlet energy	Majumdar Robbins Zyskin
35/09	A metabolite-sensitive, thermodynamically-constrained model of cardiac cross-bridge cycling: Implications for force development during ischemia	Tran Smith Loiselle Crampin
36/09	Modelling bacterial behaviour close to a no-slip plane boundary: the influence of bacterial geometry	Shum Gaffney Smith

37/09	Optimal L2-error estimates for the semidiscrete Galerkin approximation to a second order linear parabolic initial and boundary value problem with nonsmooth initial data	Goswami Pani
38/09	Optimal L2 estimates for semidiscrete Galerkin methods for parabolic integro-differential equations with nonsmooth data	Goswami Pani Yadav
39/09	Spatially structured oscillations in a two-dimensional excitatory neuronal network with synaptic depression	Kilpatrick Bressloff
40/09	Stationary bumps in a piecewise smooth neural field model with synaptic depression	Kilpatrick Bressloff
41/09	Homogenization for advection-diffusion in a perforated domain	Haynes Hoang Norris Zygalakis
42/09	Fast stochastic simulation of biochemical reaction systems by alternative formulations of the Chemical Langevin Equation	Melykuti Burrage Zygalakis
43/09	Pseudoreplication invalidates the results of many neuroscientific studies	Lazic
44/09	Cardiac cell modelling: Observations from the heart of the cardiac physiome project	Finka *et al.*
45/09	A Hybrid Radial Basis Function - Pseudospectral Method for Thermal Convection in a 3-D Spherical Shell	Wright Flyer
46/09	Refining self-propelled particle models for collective behaviour	Yates Baker Erban Maini

Copies of these, and any other OCCAM reports can be obtained from:

Oxford Centre for Collaborative Applied Mathematics
Mathematical Institute
24 - 29 St Giles'
Oxford
OX1 3LB
England
www.maths.ox.ac.uk/occam